10-1-1977

Resonance Effects and the Cepheid "Bump Mass" Anomaly

Norman R. Simon
University of Nebraska - Lincoln, nsimon@unl.edu

THE ASTROPHYSICAL JOURNAL, 217:160–170, 1977 October 1

RESONANCE EFFECTS AND THE CEPHEID "BUMP MASS" ANOMALY

NORMAN R. SIMON
Behlen Laboratory of Physics and Behlen Observatory, University of Nebraska, Lincoln
Received 1976 December 22; accepted 1977 March 30

ABSTRACT

A second-order iterative nonlinear pulsation theory is generalized to the nonadiabatic case, and employed to treat Cepheid models with linear normal-mode periods lying in the vicinity of the resonance $P_2/P_0 = 0.5$. It is shown that resonance effects occurring in the second-order terms influence the phases at which maxima appear on the theoretical velocity curves. Comparison of the iterative velocity curves with those given by hydrodynamic integration indicates good agreement in a sizable number of cases. Discrepancies which appear in a number of models are discussed. It is argued that the results of the present investigation strengthen the case for associating the bumps on Cepheid velocity curves with the resonance $P_2/P_0 = 0.5$. A brief discussion of the Cepheid "bump mass" anomaly concludes the article.

Subject headings: stars: Cepheids — stars: pulsation

I. INTRODUCTION

Comparisons between pulsational calculations and the observed properties of Cepheids allow the estimation of Cepheid masses. This information is valuable both for understanding stellar pulsations and because it provides a check on the theory of stellar evolution. Since there are several properties of Cepheids which can be used for the comparison, a number of different estimates of the mass emerge. Christy (1966*b*) and Stobie (1969*a*, *b*, *c*) obtained masses of $\frac{1}{2}$ to $\frac{2}{3}$ evolutionary by fitting the observed bumps on radial velocity curves to those obtained from fully nonlinear calculations. On the other hand, the matching of observed values of luminosity, temperature, and period to those yielded by linear pulsation analysis indicates masses for the bump Cepheids ranging from 70% to 80% of evolutionary (Fricke, Stobie, and Strittmatter 1972, hereafter FSS; Iben and Tuggle 1972; Schmidt 1973, 1975).

Iben and Tuggle (1972) have suggested that the linear pulsation masses can be raised to evolutionary values by adjustments in calibration of either luminosity or temperature, or both. Support for adjustments in luminosity has come in recent work regarding the distance of the Hyades (see Iben and Tuggle 1975). However, the discrepancy of the bump masses remains.

In an earlier paper (Simon and Schmidt 1976; hereafter SS), it was suggested that the double maximum structure of the velocity curves of bump Cepheids may be closely connected with a resonance, $P_2/P_0 \approx 0.5$, in the linear normal-mode spectrum of the corresponding models. Comparing the results of linear adiabatic calculations with the hydrodynamic integrations of Stobie (1969*b*), it was demonstrated that models with a bump on the descending branch of the theoretical velocity curve were invariably characterized by $0.53 \leq P_2/P_0 \leq 0.50$, while those with bumps on the ascending branch had $0.48 \leq P_2/P_0 \leq 0.46$. When the period ratio P_2/P_0 fell outside the range 0.53–0.46, the models showed no bumps.

If the resonance-bump relation is indeed correct, the result is important for a number of reasons. First, it provides independent confirmation of the mass anomaly emerging from the hydrodynamic integrations; second, it constitutes a new theoretical "handle" for interpreting observed velocity curves; and third, it means that physical or computational changes in the models designed to remedy the mass discrepancy can be tested first with the economical linear theory.

In view of the above considerations, it was decided to extend the work of SS by studying resonance pulsations in nonlinear, nonadiabatic Cepheid models. The vehicle chosen for this investigation was an iterative pulsation theory (Eddington 1919; Bhatnagar and Kothari 1944; Rosseland 1947; Simon 1972*a*, *b*) which calculates second-order corrections to the linear pulsation amplitudes. The corrections of interest here have a time dependence corresponding to the first harmonic of the linear perturbation. Employing this theory in adiabatic models, Simon and Sastri (1972) were able to show, both analytically and by machine integration, that in the vicinity of a resonance described by $P_j/P_0 = 0.5$ ($j = 1, 2, 3, \ldots$), the second-order correction terms are enhanced, approaching $\pm\infty$ as the resonance center is approached from different sides.

While physical intuition suggests that for nonadiabatic models the resonance effect ought to be softened but not eliminated, this can only be tested by actual calculations. We have performed such calculations with the hope that they might also shed new light on the question of the resonance-bump relationship.

In § II of the present work we generalize the iterative theory to nonadiabatic pulsations, and in § III comment upon the methods employed to solve the resulting equations. The solutions themselves are given in § IV, while § V

contains remarks regarding the functioning of the iterative approach in the present case. A final discussion of the results, including their relevance to the Cepheid bump mass anomaly, is undertaken in § VI.

II. THE ITERATIVE THEORY IN NONADIABATIC FORM

We begin with the familiar stellar equations of mass, momentum, energy and radiative transport (e.g., Cox and Giuli 1968). Convection is neglected. Following Baker and Kippenhahn (1965, hereafter BK) the dependent variables are chosen to be r, P, T, and L_r, and the independent variable to be $\ln P_0$, where P_0 is the static pressure. We write the dependent variables in the form

$$x_i = x_{0i}(1 + \delta x_i/x_{0i}) ,$$

where x_{0i} is the static value of a given variable x_i, and $\delta x_i/x_{0i}$ a small perturbation. The index i runs from 1 to 8, with the following correspondences:

$$1 \leftrightarrow \text{radius } (r) ; \quad 2 \leftrightarrow \text{density } (\rho) ; \quad 3 \leftrightarrow \text{pressure } (P) ; \quad 4 \leftrightarrow \text{temperature } (T) ;$$

$$5 \leftrightarrow \text{luminosity } (L_r) ; \quad 6 \leftrightarrow \text{opacity } (\kappa) ; \quad 7 \leftrightarrow \text{adiabatic exponent } (\Gamma_1) ;$$

$$8 \leftrightarrow \text{adiabatic exponent } (\Gamma_3) .$$

Expanding the stellar equations in binomial series, we retain terms up to second order in the quantities $\delta x_i/x_{0i}$.

Following Simon (1972*a*), the perturbations themselves are now expanded in the form of truncated Fourier series. Consistent with the quadratic approximation, these series have the form (Simon 1972*a*; Rosseland 1947; Eddington 1919)

$$\frac{\delta x_i}{x_{0i}} = A_{i0} + A_{i1} \cos \omega t - B_{i1} \sin \omega t + A_{i2} \cos 2\omega t - B_{i2} \sin 2\omega t , \qquad i = 1, 2, \ldots, 8 . \tag{1}$$

When the expressions (1) are inserted into the second-order equations, terms appear which are quadratic in the coefficients A_{i0}, A_{i1}, B_{i1}, A_{i2}, B_{i2}. Again, consistent with the order of approximation employed, all products are neglected except those involving A_{i1} and B_{i1}. Following the use of simple trigonometric identities to reexpress the terms involving $\cos^2 \omega t$, $\sin^2 \omega t$ and $\sin \omega t \cos \omega t$, the stellar equations attain a final form in which only the time dependences which appear in equation (1) are present.

We now equate coefficients of corresponding Fourier terms. The set of equations arising from the time-independent terms and involving the A_{i0} do not concern us here. They have been treated in the adiabatic case by Simon (1971, 1972*b*) and Simon and Sastri (1972). Equating the coefficients of $\cos \omega t$ and those of $\sin \omega t$ yields the following set of eight equations in the A_{i1} and B_{i1}:

$$\begin{aligned}
A_{11}' - F_1(3A_{11} + \rho_P A_{31} + \rho_T A_{41}) &= 0 , \\
B_{11}' - F_1(3B_{11} + \rho_P B_{31} + \rho_T B_{41}) &= 0 , \\
A_{31}' + A_{31} + [4 + (3\sigma^2 x^3/q)]A_{11} &= 0 , \\
B_{31}' + B_{31} + [4 + (3\sigma^2 x^3/q)]B_{11} &= 0 , \\
A_{41}' + \nabla_{\text{rad}}[4A_{11} + (4 - \kappa_T)A_{41} - \kappa_P A_{31} - A_{51}] &= 0 , \\
B_{41}' + \nabla_{\text{rad}}[4B_{11} + (4 - \kappa_T)B_{41} - \kappa_P B_{31} - B_{51}] &= 0 , \\
A_{51}' - \sigma F_2[(B_{41}/\nabla_{\text{ad}}) - B_{31}] &= 0 , \\
B_{51}' + \sigma F_2[(A_{41}/\nabla_{\text{ad}}) - A_{31}] &= 0 ,
\end{aligned} \tag{2}$$

where a prime indicates differentiation with respect to $\ln P_0$, all quantities apart from the A_{i1} and B_{i1} refer to the static model, and we further define

$$F_1 = \frac{rP}{\rho G m} , \qquad F_2 = \frac{4\pi P^2 r^4 \rho_T}{Lm\rho} \left(\frac{3M}{GR^3}\right)^{1/2} , \qquad \sigma^2 = \frac{\omega^2 R^3}{3GM} , \qquad \kappa_T = \left.\frac{\partial \ln \kappa}{\partial \ln T}\right|_P , \qquad \kappa_P = \left.\frac{\partial \ln \kappa}{\partial \ln P}\right|_T ,$$

$$\rho_T = \left.\frac{\partial \ln \rho}{\partial \ln T}\right|_P , \qquad \rho_P = \left.\frac{\partial \ln \rho}{\partial \ln P}\right|_T .$$

All other quantities have their standard meanings (see, e.g., BK).

When the A_{i1} and B_{i1} are respectively associated with the real and imaginary parts of the various perturbations, the eight equations (2) are identical with the standard linear nonadiabatic equations (BK), provided that the latter

are considered in the limit $\sigma_i/\sigma_r = 0$. Since this ratio is of the order of 1% in the models studied, the difference between the two sets of equations is, for our purposes, negligible.

We now equate the coefficients of $\cos 2\omega t$ and $\sin 2\omega t$, obtaining a set of eight coupled equations which are linear in the second-order corrections A_{i2}, B_{i2} ($i = 1, 2, \ldots, 8$). These equations are as follows:

$$A_{12}' - F_1(3A_{12} + \rho_P A_{32} + \rho_T A_{42}) = D_1\,, \tag{3}$$

$$B_{12}' - F_1(3B_{12} + \rho_P B_{32} + \rho_T B_{42}) = E_1\,, \tag{4}$$

$$A_{32}' + A_{32} + 4\left[\frac{3\sigma^2 x^3}{q} + 1\right]A_{12} = D_3\,, \tag{5}$$

$$B_{32}' + B_{32} + 4\left[\frac{3\sigma^2 x^3}{q} + 1\right]B_{12} = E_3\,, \tag{6}$$

$$A_{42}' + \nabla_{\rm rad}[4A_{12} + (4 - \kappa_T)A_{42} - \kappa_P A_{32} - A_{52}] = D_4\,, \tag{7}$$

$$B_{42}' + \nabla_{\rm rad}[4B_{12} + (4 - \kappa_T)B_{42} - \kappa_P B_{32} - B_{52}] = E_4\,, \tag{8}$$

$$A_{52}' - 2\sigma F_2[(B_{42}/\nabla_{\rm ad}) - B_{32}] = D_5\,, \tag{9}$$

$$B_{52}' + 2\sigma F_2[(A_{42}/\nabla_{\rm ad}) - A_{32}] = E_5\,. \tag{10}$$

The right-hand sides of equations (3)–(10) contain products of the linear amplitudes A_{i1}, B_{i1} ($i = 1, 2, \ldots, 8$). The expressions are

$$D_1 = \tfrac{1}{2}F_1[\tfrac{1}{2}\rho_{PP}(A_{31}^2 - B_{31}^2) + \tfrac{1}{2}\rho_{TT}(A_{41}^2 - B_{41}^2) + \rho_{PT}(A_{31}A_{41} - B_{31}B_{41}) + B_{21}^2 + 2B_{11}B_{21} + 3B_{11}^2 - A_{21}^2 - 2A_{11}A_{21} - 3A_{11}^2]\,, \tag{11}$$

$$E_1 = \tfrac{1}{2}F_1[\rho_{PP}A_{31}B_{31} + \rho_{TT}A_{41}B_{41} + \rho_{PT}(A_{31}B_{41} + B_{31}A_{41}) - 2A_{21}B_{21} - 2B_{11}A_{21} - 2A_{11}B_{21} - 6A_{11}B_{11}]\,, \tag{12}$$

$$D_3 = B_{11}B_{31} - B_{11}^2 - A_{11}A_{31} + A_{11}^2 + B_{11}B_{31}' - A_{11}A_{31}'\,, \tag{13}$$

$$E_3 = 2A_{11}B_{11} - A_{11}B_{31} - B_{11}A_{31} - A_{11}B_{31}' - B_{11}A_{31}'\,, \tag{14}$$

$$D_4 = \tfrac{1}{2}\nabla_{\rm rad}[\tfrac{1}{2}\kappa_{PP}(A_{31}^2 - B_{31}^2) + \tfrac{1}{2}\kappa_{TT}(A_{41}^2 - B_{41}^2) + \kappa_{PT}(A_{31}A_{41} - B_{31}B_{41}) + 6B_{41}^2 + B_{61}^2 - 4B_{41}B_{61} + 16B_{11}B_{41} - 4B_{11}B_{61} + 6B_{11}^2 - 6A_{41}^2 - A_{61}^2 + 4A_{41}A_{61} - 16A_{11}A_{41} + 4A_{11}A_{61} - 6A_{11}^2] + \tfrac{1}{2}[B_{41}'(3B_{41} - B_{61} + 4B_{11}) - A_{41}'(3A_{41} - A_{61} + 4A_{11})]\,, \tag{15}$$

$$E_4 = \tfrac{1}{2}\nabla_{\rm rad}[\kappa_{PP}A_{31}B_{31} + \kappa_{TT}A_{41}B_{41} + \kappa_{PT}(A_{31}B_{41} + B_{31}A_{41}) - 12A_{41}B_{41} - 2A_{61}B_{61} + 4A_{41}B_{61} + 4B_{41}A_{61} - 16A_{11}B_{41} - 16B_{11}A_{41} + 4A_{11}B_{61} + 4B_{11}A_{61} - 12A_{11}B_{11}] - \tfrac{1}{2}[A_{41}'(3B_{41} - B_{61} + 4B_{11}) + B_{41}'(3A_{41} - A_{61} + 4A_{11})]\,, \tag{16}$$

$$D_5 = \frac{\sigma F_2}{\rho_T \nabla_{\rm ad}}[\rho_{PP}A_{31}B_{31} + \rho_{TT}A_{41}B_{41} + \rho_{PT}(A_{31}B_{41} + B_{31}A_{41}) + \tfrac{1}{2}B_{21}(A_{71} + A_{31} - A_{21}) + \tfrac{1}{2}A_{21}(B_{71} + B_{31} - B_{21})] + \tfrac{1}{2}B_{51}'\left[\frac{\Gamma_3}{\Gamma_3 - 1}B_{81} + B_{21}\right] - \tfrac{1}{2}A_{51}'\left[\frac{\Gamma_3}{\Gamma_3 - 1}A_{81} + A_{21}\right]\,, \tag{17}$$

$$E_5 = -\frac{1}{2}\frac{\sigma F_2}{\rho_T \nabla_{\rm ad}}[\rho_{PP}(A_{31}^2 - B_{31}^2) + \rho_{TT}(A_{41}^2 - B_{41}^2) + 2\rho_{PT}(A_{31}A_{41} - B_{31}B_{41}) + A_{21}(A_{71} + A_{31} - A_{21}) - B_{21}(B_{71} + B_{31} - B_{21})] - \tfrac{1}{2}A_{51}'\left[\frac{\Gamma_3}{\Gamma_3 - 1}B_{81} + B_{21}\right] - \tfrac{1}{2}B_{51}'\left[\frac{\Gamma_3}{\Gamma_3 - 1}A_{81} + A_{21}\right]\,. \tag{18}$$

Here we have

$$\rho_{PP} = \frac{P^2}{\rho}\frac{\partial^2\rho}{\partial P^2}, \qquad \rho_{TT} = \frac{T^2}{\rho}\frac{\partial^2\rho}{\partial T^2}, \qquad \rho_{PT} = \frac{PT}{\rho}\frac{\partial^2\rho}{\partial P\partial T},$$

and

$$\kappa_{PP} = \frac{P^2}{\kappa}\frac{\partial^2\kappa}{\partial P^2}, \qquad \kappa_{TT} = \frac{T^2}{\kappa}\frac{\partial^2\kappa}{\partial T^2}, \qquad \kappa_{PT} = \frac{PT}{\kappa}\frac{\partial^2\kappa}{\partial P\partial T}.$$

The expressions (11)–(18) may be evaluated from the linear solution with the aid of the auxiliary relations which follow:

$$A_{21} = \rho_P A_{31} + \rho_T A_{41},$$

$$B_{21} = \rho_P B_{31} + \rho_T B_{41},$$

$$A_{22} = \rho_P A_{32} + \rho_T A_{42} + \tfrac{1}{4}\rho_{PP}(A_{31}^2 - B_{31}^2) + \tfrac{1}{4}\rho_{TT}(A_{41}^2 - B_{41}^2) + \tfrac{1}{2}\rho_{PT}(A_{31}A_{41} - B_{31}B_{41}),$$

$$B_{22} = \rho_P B_{32} + \rho_T B_{42} + \tfrac{1}{2}\rho_{PP}A_{31}B_{31} + \tfrac{1}{2}\rho_{TT}A_{41}B_{41} + \tfrac{1}{2}\rho_{PT}(A_{31}B_{41} + B_{31}A_{41}),$$

$$A_{61} = \kappa_P A_{31} + \kappa_T A_{41},$$

$$B_{61} = \kappa_P B_{31} + \kappa_T B_{41},$$

$$A_{62} = \kappa_P A_{32} + \kappa_T A_{42} + \tfrac{1}{4}\kappa_{PP}(A_{31}^2 - B_{31}^2) + \tfrac{1}{4}\kappa_{TT}(A_{41}^2 - B_{41}^2) + \tfrac{1}{2}\kappa_{PT}(A_{31}A_{41} - B_{31}B_{41}),$$

$$B_{62} = \kappa_P B_{32} + \kappa_T B_{42} + \tfrac{1}{2}\kappa_{PP}A_{31}B_{31} + \tfrac{1}{2}\kappa_{TT}A_{41}B_{41} + \tfrac{1}{2}\kappa_{PT}(A_{31}B_{41} + B_{31}A_{41}),$$

$$A_{71} = (\partial \ln \Gamma_1/\partial \ln P)A_{31} + (\partial \ln \Gamma_1/\partial \ln T)A_{41},$$

$$B_{71} = (\partial \ln \Gamma_1/\partial \ln P)B_{31} + (\partial \ln \Gamma_1/\partial \ln T)B_{41},$$

$$A_{81} = (\partial \ln \Gamma_3/\partial \ln P)A_{31} + (\partial \ln \Gamma_3/\partial \ln T)A_{41},$$

$$B_{81} = (\partial \ln \Gamma_3/\partial \ln P)B_{31} + (\partial \ln \Gamma_3/\partial \ln T)B_{41}.$$

III. SOLUTION OF THE EQUATIONS

a) The Linear Equations

Static Cepheid envelopes were generated as in SS, employing the thermodynamics of Stobie (1969*a*) and the analytic opacity formula of Christy (1966*a*). The atmospheres were similar to those of Iben (1971) except that T_e was taken to be $2^{1/4}T_0$.

Since the difference between equations (2) and the familiar linear nonadiabatic pulsation equations (BK) may be neglected in the present case (see § II), it was decided to solve the latter set in order to facilitate checking of the computer program. "Standard" boundary conditions were employed as described by Iben (1971), with the real and imaginary parts of $\delta r/r$ taken to be unity and zero, respectively, at the surface. The technique used for the integrations was similar to that of Iben in that iteration was performed over both eigenvalues and eigenfunctions. The Sherman-Morrison formula (Householder 1964) was employed in the algorithm to reduce the problem to one involving band matrices only. A number of RR Lyrae pulsation models, integrated as tests, showed good agreement with the corresponding models of Iben (1971).

The linear nonadiabatic Cepheid results were used to generate expressions (11)–(18). In this process, the A_{i1} and B_{i1} ($i = 1, 2, \ldots, 8$) are equal, respectively, to the real and imaginary parts of the corresponding eigenfunctions. With phases taken in the manner of Iben (1971), this correspondence is: $A_{11} = x_r$, $B_{11} = x_i$; $A_{31} = p_r$, $B_{31} = p_i$; $A_{41} = t_r$, $B_{41} = t_i$; $A_{51} = l_r$, $B_{51} = l_i$. The quantity σ is the real part of the angular frequency, written in dimensionless form.

b) Boundary Conditions

Once their right-hand sides are known, equations (3)–(10) may be solved for the eight quantities A_{i2}, B_{i2} ($i = 1, 3, 4, 5$). Consistent with the linear case, boundary conditions in the interior were taken to be

$$A_{12} = B_{12} = A_{52} = B_{52} = 0; \tag{19}$$

i.e., the variations of radius and luminosity were made to vanish.

At the surface the thermal boundary conditions were derived from the expression

$$L = 2\pi acR^2T^4 .$$

Expansion of this relation to second order in pulsational quantities, followed by insertion of Fourier series as above, yields the "standard" linear boundary conditions along with the nonlinear relations

$$A_{52} = 2A_{12} + 4A_{42} + \tfrac{1}{2}(6A_{41}^2 + A_{11}^2 + 8A_{11}A_{41} - 6B_{41}^2 - B_{11}^2 - 8B_{11}B_{41}) , \tag{20}$$

$$B_{52} = 2B_{12} + 4B_{42} + 6A_{41}B_{41} + A_{11}B_{11} + 4A_{11}B_{41} + 4B_{11}A_{41} . \tag{21}$$

To derive mechanical boundary conditions at the surface, we have chosen to employ the "quasi-equilibrium" relation given by Unno (1965):

$$\frac{P}{P_0} = \left(\frac{R_0}{R}\right)^4\left[1 + \frac{R^2\ddot{R}}{GM}\right] ,$$

where P_0 and R_0 refer to static values. Once again we expand to second order and equate Fourier terms to obtain the standard linear boundary conditions, along with the nonlinear conditions

$$A_{32}' = B_{32}' = 0 . \tag{22}$$

Equations (19)–(22) provide the needed set of eight boundary conditions. Their virtues are the minimum ones—namely, they are consistent with the linear conditions and easy to obtain. No attempt was made in this investigation to employ alternative boundary conditions.

c) *The Second-Order Equations*

The technique adopted to solve equations (3)–(10) was similar to that used for the linear equations. The model was divided into discrete shells and the equations differenced, the right-hand sides being evaluated in the form of averages between contiguous shells. A model with N shells yields $8(N - 1)$ linear algebraic equations in the $8(N - 1)$ variables which remain after the boundary conditions eliminate the corrections to A_{12}, B_{12}, A_{52}, and B_{52} at the interior boundary, and the corrections to A_{52}, B_{52}, A_{32}, and B_{32} at the surface. Since the second-order equations do not contain eigenvalues, the matrix describing the system is a band matrix, easily handled by standard techniques. Approximately 400 shells were necessary for the calculation of a typical model.

IV. RESULTS OF THE CALCULATIONS

a) *Appearance of the Resonance*

Two model series were calculated, each at constant mass and luminosity. The first series is characterized by $M = 8\ M_\odot$, $L = 10^4\ L_\odot$ ($L_\odot = 3.826 \times 10^{33}$ ergs s^{-1}), and may be compared with the models numbered "8" in the second survey of Stobie (1969*b*). The composition is $X = 0.66$, $Z = 0.04$. The second series has $M = 4\ M_\odot$, $L = 3249\ L_\odot$, and includes the "Goddard model" (Fischel and Sparks 1975). Its composition is $X = 0.70$, $Z = 0.02$.

In the present (i.e., second-order) version of the iterative theory, each pulsational perturbation is approximated by the first two terms of a Fourier series, e.g.,

$$\frac{\delta r}{r} = A_{11}\cos\omega t - B_{11}\sin\omega t + A_{12}\cos 2\omega t - B_{12}\sin 2\omega t .$$

For convenience, we rewrite this in the form

$$\frac{\delta r}{r} = \alpha_r\cos(\omega t + \phi_{r1}) + \beta_r\cos(2\omega t + \phi_{r2}) . \tag{23}$$

Similarly, we shall write

$$\frac{\delta P}{P} = \alpha_p\cos(\omega t + \phi_{p1}) + \beta_p\cos(2\omega t + \phi_{p2}) ,$$

$$\frac{\delta T}{T} = \alpha_t\cos(\omega t + \phi_{t1}) + \beta_t\cos(2\omega t + \phi_{t2}) ,$$

$$\frac{\delta L_r}{L_r} = \alpha_l\cos(\omega t + \phi_{l1}) + \beta_l\cos(2\omega t + \phi_{l2}) .$$

TABLE 1

LINEAR PULSATION CHARACTERISTICS FOR SELECTED MODELS

Model No.	T_{eff}	P_0* (days)	$100\sigma_l/\sigma_r$	α_t	ϕ_{t1}†	α_l	ϕ_{l1}†
			$M = 8\ M_\odot, L = 10^4\ L_\odot$				
81.....	5850	14.5	−0.009	16.3	135	5.72	110
82.....	5750	15.4	−0.184	14.8	130	5.34	101
8b.....	5600	17.0	−0.514	12.4	121	4.74	84.5
83.....	5450	18.8	−0.836	10.5	114	4.31	69.2
8c.....	5300	20.9	−1.21	7.90	106	3.86	52.2
84.....	5150	23.5	−1.38	6.24	100	3.67	40.5
8d.....	5000	26.5	−1.50	4.57	94	3.50	28.9
			$M = 4\ M_\odot, L = 3249\ L_\odot$				
41.....	6000	8.03	−0.089	15.1	135	5.57	109
42.....	5800	9.10	−0.534	12.3	125	4.80	90.1
43.....	5700	9.71	−0.796	10.8	120	4.44	79.5
44.....	5550	10.8	−1.19	8.70	113	3.99	63.6
45.....	5500	11.2	−1.33	8.06	111	3.87	57.7
46.....	5300	12.9	−1.64	5.79	104	3.55	41.5
47.....	5200	14.0	−1.79	4.59	99.9	3.42	32.6

* Linear nonadiabatic period.

† Measured in degrees from maximum radius.

Table 1 gives some linear results for a representative selection of models. The amplitudes are scaled to the value $\alpha_r = 1.0$ at the surface of each model.

The nonlinear results are presented in Figures 1–4, where the second-order surface amplitudes β_j ($j = r, p, t, l$) and phases $\Delta\phi_j \equiv \phi_{j2} - 2\phi_{j1}$ are plotted against fundamental period for each of the two model series. The right-

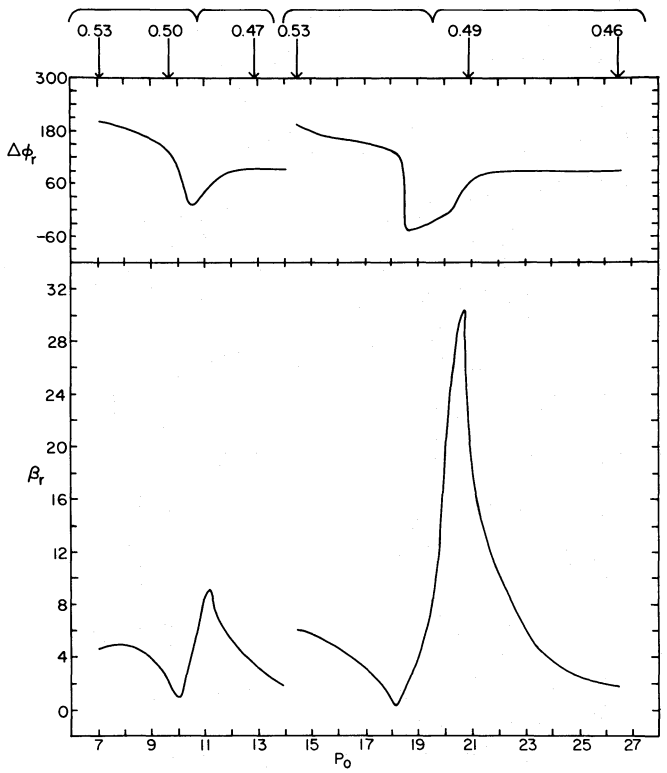

FIG. 1.—Amplitude (β_r) and phase shift ($\Delta\phi_r \equiv \phi_{r2} - 2\phi_{r1}$) of the second-order corrections to the linear radius amplitude. *Left side*, 4 $M_\odot$ series; *right side*, 8 $M_\odot$ series. Arrows at top of figure indicate adiabatic ratio P_2/P_0.

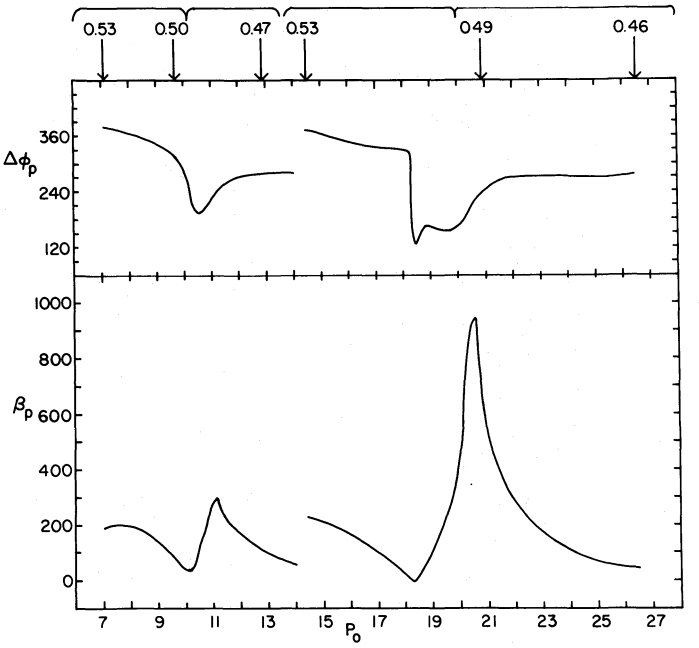

FIG. 2.—Same as Fig. 1, except that second-order corrections to pressure amplitude are plotted

hand curves in each figure represent the 8 $M_\odot$ models, the left-hand curves the 4 $M_\odot$ models. Arrows at the tops of the figures indicate values of the adiabatic period ratio P_2/P_0 for each series.

In both Table 1 and Figures 1–4, the amplitudes and phases of radius and pressure variations have been evaluated in the vicinity of $\tau = 0.2$, while corresponding quantities for temperature and luminosity refer to the photosphere ($\tau = \frac{2}{3}$).

From Figures 1–4, it is clear that for both series the amplitudes and phases of the second-order terms undergo abrupt changes in the vicinity of the resonance center, $P_2/P_0 = 0.5$. (Actually the midpoint of the change is, as suggested in SS, more nearly located at $P_2/P_0 = 0.49$.) We notice that the changes are more pronounced in the "mechanical" variables r and P than in the "thermal" variables T and L_r. This is in line with our understanding of the resonance effects as essentially "adiabatic" in nature, i.e., as depending upon a ratio of periods which is determined largely in the adiabatic interior.

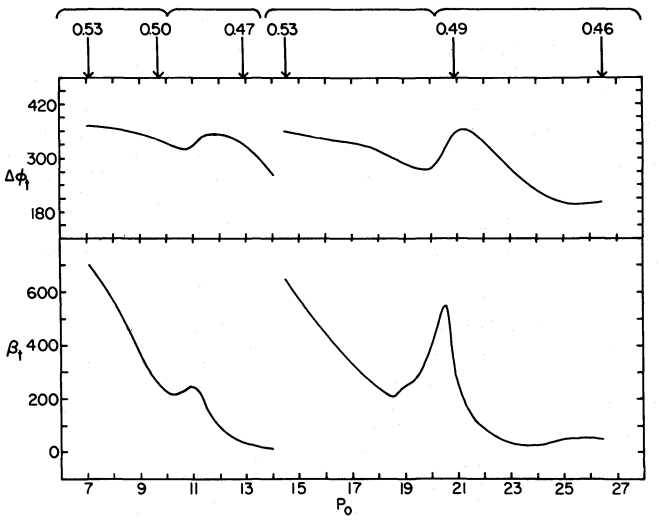

FIG. 3.—Same as Fig. 1, except that second-order corrections to temperature amplitude are plotted

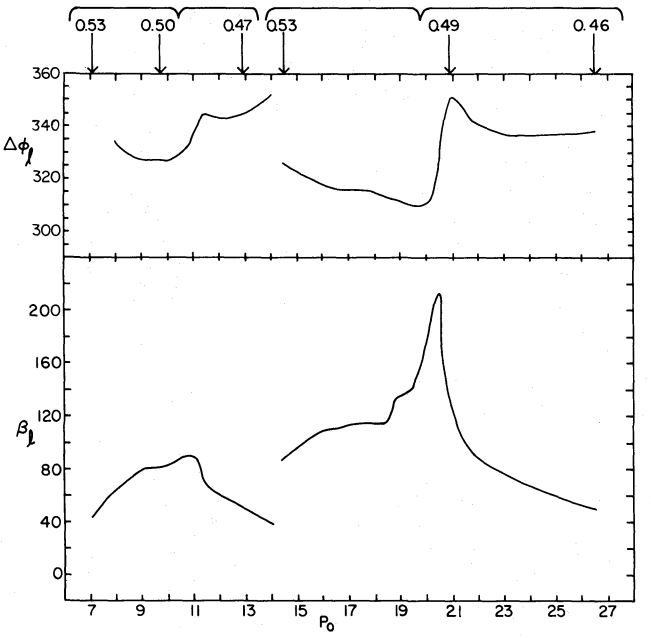

FIG. 4.—Same as Fig. 1, except that second-order corrections to luminosity amplitude are plotted

It may also be seen from the figures that the resonance is much sharper in the 8 $M_\odot$ series as compared with the 4 $M_\odot$ series. At the present time, we have not integrated enough additional models to be able to tell how much of this distinction is contributed by mass and how much by radius.

b) The Velocity Curves

Having established that the resonance effect does appear in the nonadiabatic models studied, we turn now to an examination of the velocity curves generated by the truncated Fourier series (23).

The velocity is obtained by simple differentiation:

$$v = -\lambda r_0 \omega [\alpha_r \sin(\omega t + \phi_{r1}) + 2\lambda\beta_r \sin(2\omega t + \phi_{r2})] . \quad (24)$$

We note in this expression the scale factor λ, which has been inserted to emphasize that the iterative theory, like the linear theory, is arbitrary to within such a factor—the linear amplitude α_r scaling like λ, the nonlinear correction β_r like λ^2 (Simon 1972*a*). This scale factor must be fixed from outside the theory, e.g., by imposing an observed velocity amplitude, or a limiting amplitude obtained from full hydrodynamic calculations.

A brief comparison of velocity curves generated by us, with those given by Stobie (1969*b*) for the same models, has already been published elsewhere (Simon 1976). The situation is that for "bump" Cepheid models on the hot (short period) side of a given resonance center there is good (if crude) agreement between the iterative and hydrodynamic calculations as to the phases of the two maxima. As one proceeds through the resonance center to the cool (long period) models of a given series, the iterative theory departs more and more from the results of hydrodynamic integrations and presumably also from those of observations.

The results are summarized in Figures 5 and 6, which are plots of the product of period and phase of maximum velocity versus model radius in solar units (FSS). The velocity maximum is always measured with respect to minimum radius.

In Figure 5, the phase ϕ refers to the *second* (but not necessarily secondary) maximum of velocity. The straight line comes from FSS, and represents the results of hydrodynamic integrations (Stobie 1969*b*). The circles are data from the present investigation, including a handful of extra models not part of the 8 $M_\odot$ or 4 $M_\odot$ series. Open circles indicate models for which $P_2/P_0 > 0.49$; filled circles, models for which $P_2/P_0 \leq 0.49$. As mentioned above, one sees that the short-period iterative models agree well with the hydrodynamic results while the long-period models begin to depart drastically.

Figure 6 treats the phase of the *first* (but not necessarily primary) velocity maximum. Data from the present work are presented as in Figure 5. The straight line has a slope 0.2 and represents an eyeball fit to points given by FSS. (However, note that whereas these authors have only plotted the first maxima when they were *secondary*, we have plotted them in all cases.) One sees from Figure 6 that the first maximum seems to follow the straight-line relationship fairly well, except for a few models far to the long-period side of the resonance center.

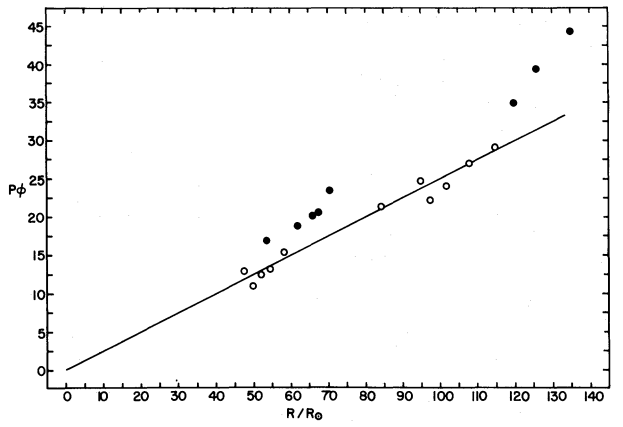

FIG. 5

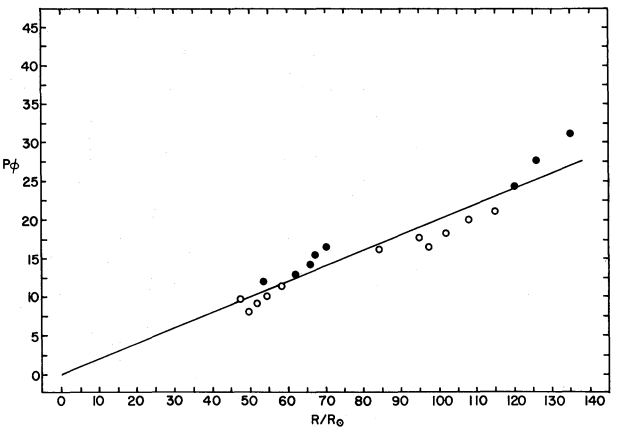

FIG. 6

FIG. 5.—The product $P\phi$ versus radius in solar units, following FSS. P is fundamental period; ϕ is phase of second maximum in velocity curves. Solid line indicates locus of second maxima for velocity curves of Stobie (1969*b*). Circles refer to present investigation. *Open circles*, models for which $P_2/P_0 > 0.49$; *filled circles*, $P_2/P_0 \leq 0.49$. Period ratios are adiabatic.

FIG. 6.—Same as Fig. 5, except that data refer to first maximum in velocity curves.

V. REMARKS ON THE ITERATIVE THEORY

a) Bump or No Bump?

As discussed in § IV*b*, velocity data from the iterative theory require for their interpretation the assignment of a value to the scale factor λ. For the data in Figures 5 and 6 this was sometimes done with the aid of limiting amplitudes from Stobie (1969*b*), and was sometimes done arbitrarily. The justification for the arbitrary assignments is that for all reasonable amplitudes, the *phases* of the velocity maxima turn out to depend only very weakly on $\lambda\beta_r$, their values being determined essentially by the phase shift $\Delta\phi_r = \phi_{r2} - 2\phi_{r1}$, which is independent of λ.

When values of λ were assigned arbitrarily, it was for one of two reasons: (1) no limiting amplitudes were available; or (2) the limiting amplitudes given by Stobie were too small to produce a double maximum in the iterative velocity curves.

The second circumstance may be made clearer by an examination of equation (24). The shape of the velocity curve will depend upon the phase difference $\Delta\phi_r$ and upon the amplitude ratio $2\lambda\beta_r/\alpha_r$. Since for all models integrated the linear amplitude α_r (fixed at unity at the surface) had, at $\tau = 0.2$, a value in the range $0.86 \leq \alpha_r \leq 0.92$, the amplitude ratio was essentially independent of α_r. In the limit $\lambda\beta_r \to 0$ the velocity curve becomes, of course, sinusoidal. For nonzero $\lambda\beta_r$ below a threshold value, $\lambda_{\text{thresh}}\beta_r$, the curve will be asymmetric, but with a single maximum. Only when $\lambda\beta_r$ exceeds $\lambda_{\text{thresh}}\beta_r$ will the double-maximum structure be realized, and in that case the phases of the maxima will vary little with increasing λ over a wide range. For example, in the models studied $0.15 \lesssim \lambda_{\text{thresh}}\beta_r \lesssim 0.25$, depending on the value of $\Delta\phi_r$, while the phases of the velocity maxima, as expressed by the product $P\phi$, changed by only a few percent even for values of $\lambda\beta_r$ as high as 0.45. Velocity amplitudes for the models plotted in Figures 5 and 6 ranged between 27 and 90 km s^{-1}, with most of them concentrated between 30 and 50 km s^{-1}.

Let us summarize in the following way the comparison between the hydrodynamic and iterative results for limiting amplitude velocity curves. With regard to the *appearance or nonappearance* of a bump (i.e., a second maximum), the iterative theory fails to reproduce the hydrodynamic results (in the sense that no bump appears in the former) in a number of models lying largely in the vicinity of a minimum in β_r which precedes its sharp rise at the resonance center (see Fig. 1). With regard to the *phases* of the two maxima, the iterative and hydrodynamic results agree quite well, except for the cooler models in each series.

b) The Higher-Order Terms

The results of the iterative approach versus the hydrodynamic may be viewed from two different perspectives. On the one hand one may ask why the iterative theory does not reproduce the hydrodynamic results better; on the other, one may be surprised that it reproduces them as well as it does.

Let us examine the latter point first. In the Fourier analysis of a periodic function, the presence of maxima may be associated, at least in crude approximation, with the strengths of various harmonics. Thus, a Fourier series containing the fundamental frequency only (say, ω) produces a curve with a single maximum; if a sizable contribution of first harmonic (2ω) is added, the curve will then have two maxima (see § V*a*); if the second harmonic (3ω) plays an important role, there will be three maxima, etc. From this point of view, we see that the very fact that the

bump Cepheid velocity curves exhibit a double-maximum structure indicates that a two-term Fourier approximation ought to be at least crudely successful in describing them.

We now turn to the question of the shortcomings of the iterative results vis-à-vis the hydrodynamic. The obvious disadvantage of the iterative theory lies in the truncation of the Fourier series following the first harmonic. While the appeal to "higher-order terms" is capable of covering a multitude of sins, we would nonetheless like to touch briefly on the question of what an extension of the iterative theory might be expected to produce.

In the next order of approximation in the iterative approach (Simon 1972*a*), a second-harmonic term (i.e., cos $3\omega t$) appears, as well as a correction to the linear term (cos ωt). The cos $2\omega t$ term is left unchanged. Referring to equation (24), one sees that this means that in the next order both the amplitude ratio $2\lambda\beta_r/\alpha_r$ and the phase difference $\Delta\phi_r$ will undergo changes.

It is relatively easy to account for the fact that phase predictions in the iterative theory begin to go awry in the cooler models of each series. Stobie (1969*b*) has shown that limiting amplitudes are large for these models, which in turn suggests that higher-order harmonics ought to play an enhanced role. It turns out, in fact, that it is impossible to duplicate, even crudely, a typical velocity curve of Stobie's type A (bump on ascending branch; sharp rise to first maximum followed by sharp rise to second maximum; e.g., the model 7d, Fig. 6, Stobie 1969*b*) with a Fourier series truncated after the first harmonic.

On the other hand, the case of model 8b (Stobie 1969*b*) is more difficult to understand. Whereas Stobie gives the limiting amplitude for the model as 27 km s^{-1}, the double maximum does not appear in the iterative version until the amplitude has reached 65 km s^{-1}. (Again, when the two maxima do appear, their phases are correct.) To explain this by the intervention of higher-order terms one must postulate a third-order correction which raises the ratio β_r/α_r (by lowering α_r) yet leaves ϕ_{r1}, and thus $\Delta\phi_r$, intact so as not to destroy the phases, which are already correct. Whether or not the third-order correction indeed has such a form remains to be seen.

We close this section by remarking that the best comparison between the iterative and hydrodynamic results would actually be in terms of the radial extension ($\delta r/r$), rather than the velocity. The reason is simply that differentiation of the Fourier series $\sum a_n \cos n\omega t$ brings down the factor n, a circumstance which enhances the harmonics vis-à-vis the fundamental, and the higher harmonics vis-à-vis the lower ones. Unfortunately, radial extension data from hydrodynamic calculations are not readily available.

VI. DISCUSSION

In this section, we wish to briefly reexamine the question of the resonance-bump relation in light of the data from the present investigation. We shall begin with a heuristic description of the pulsational effects of the resonance. For this purpose it is convenient to conceptually divide the system into a series of "natural oscillator frequencies" on the one hand, and a set of "external driving frequencies" on the other. Consider, then, a Cepheid with a linearly unstable fundamental mode. The external driving frequencies consist in this case of the fundamental and all of its harmonics. The natural oscillator frequencies are the fundamental and all of the other linear normal modes. When the circumstance arises that one of the harmonics (external driving frequencies) corresponds closely in frequency with one of the normal modes (natural oscillator frequencies), the oscillation is enhanced at the frequency of the driving harmonic in question. The nonlinear pulsation may then be thought of as a superposition of all the (spatially weighted) harmonic frequencies, i.e., a Fourier series.

For the models presently under investigation (i.e., for $P_2/P_0 \approx 0.5$), the harmonic in question is the first harmonic, and the normal mode the second overtone. The double-maximum structure of the oscillation is attributed to a superposition of amplitudes at the frequencies ω and 2ω. Note that it is not necessary to require the exact commensurability of the fundamental and second overtone frequencies in order to avoid drifting, since it is the fundamental and *first harmonic* frequencies that combine to produce the bump structure. In the language of elementary mechanics, a forced oscillator persists not at its natural frequency but rather at the frequency of the driving force.

It should be emphasized that the foregoing description, by no means exhaustive or complete, is meant only as a qualitative picture of the resonance effects. It says nothing at all regarding such pivotal considerations as the spatial construction of the pulsation, interference between driving frequencies, the dynamic mechanism for producing the bump, etc. Nonetheless, we believe that the results of the present investigation strengthen the case for associating the Cepheid bumps with the resonance $P_2/P_0 = 0.5$. We have shown that resonance effects do indeed appear in nonadiabatic Cepheid models, that these effects influence the phases of velocity maxima, and that the second-order iterative theory is often capable of predicting where the two maxima will occur.

While the resonance explanation for the Cepheid bumps seems to predict unerringly (SS) which models will show the double maximum, it tells us nothing about the dynamical mechanism for actually producing the bumps. The reflected pressure wave theory (Christy 1967) provides such a dynamical mechanism, but fails to predict the phases of the bumps, or to explain why the mechanism works in some models but not in others. Thus the two descriptions, certainly not *a priori* in conflict, may turn out to be complementary.

In any event, the situation at present is that four diverse theoretical approaches (hydrodynamic, after Christy 1966*a*; hydrodynamic, after Stellingwerf 1974; linear, as in SS; and iterative, as in the present investigation) all converge on the unsettling result that Cepheid bumps indicate masses substantially lower than evolutionary. When this finding is combined with a similar mass anomaly indicated for the double-mode Cepheids (e.g., Cox *et al.*

1977), a fundamental and serious gap opens between the results of stellar pulsation theory and those of the theory of stellar evolution.

To be sure, the relatively "painless" closing of this gap could be accomplished by the mechanism of mass loss. However, in that case, not only would the amount of discarded matter need to be very large, but, as indicated by the great regularity of the bump Cepheids in the period-luminosity diagram (see SS), the mass-ejection mechanism would have to be extremely precise in order that single-maximum Cepheids not be placed in the bump region or vice versa.

In the absence of such heavy yet delicate mass loss, one is faced with the possibility that nontrivial revisions may need to be made in pulsation theory, evolution theory, or both. The substantial agreement of diverse pulsation theories that there is a Cepheid mass discrepancy indicates that if a commonly held error is at fault, it is likely to be a deep-seated one. Similarly, it does not seem that minor changes in the theory of stellar evolution could account for a mass anomaly that may be as high as 50%. Should the problem lie in the physics of the stellar interior, both pulsations and evolution are likely to be affected. Solution of the Cepheid mass problem ought to go a long way toward improving our understanding not only of stellar pulsations but perhaps also of the intermediate stages of stellar evolution.

This investigation was begun at the NASA–Ames Research Center under the tenure of a Maude Hammond Fling Summer Faculty Fellowship from the University of Nebraska Foundation. The author wishes to thank Ray Reynolds for his hospitality at the Theoretical Studies Branch of NASA–Ames, and Dave Galant (also of NASA–Ames) for his extremely helpful suggestions regarding numerical analysis. A portion of the present work has already been reported to the Solar and Stellar Pulsation Conference at the Los Alamos Scientific Laboratory. Interesting and informative discussions with a number of the participants are gladly acknowledged.

REFERENCES

Baker, N., and Kippenhahn, R. 1965, *Ap. J.*, **142**, 868 (BK).
Bhatnagar, P. L., and Kothari, D. S. 1944, *M.N.R.A.S.*, **104**, 292.
Christy, R. F. 1966*a*, *Ap. J.*, **144**, 108.
———. 1966*b*, *Ap. J.*, **145**, 340.
———. 1967, in *Aerodynamical Phenomena in Stellar Atmospheres*, ed. R. N. Thomas (London: Academic Press), p. 105.
Cox, A. N., King, D. S., Hodson, S. W., and Henden, A. A. 1977, *Ap. J.*, **212**, 451.
Cox, J. P., and Giuli, R. T. 1968, *Principles of Stellar Structure* (New York: Gordon & Breach).
Eddington, A. S. 1919, *M.N.R.A.S.*, **79**, 177.
Fischel, D., and Sparks, W. M., eds. 1975, *Proceedings of the Cepheid Modeling Conference and Workshop* (NASA: SP-383).
Fricke, K., Stobie, R. S., and Strittmatter, P. A. 1972, *Ap. J.*, **171**, 593 (FSS).
Householder, A. S. 1964, *Theory of Matrices in Numerical Analysis* (New York: Blaisdell), p. 123.
Iben, I. 1971, *Ap. J.*, **166**, 131.
Iben, I., and Tuggle, R. S. 1972, *Ap. J.*, **173**, 135.
———. 1975, *Ap. J.*, **197**, 39.
Rosseland, S. 1949, *The Pulsation Theory of Variable Stars* (Oxford: Clarendon Press).
Schmidt, E. G. 1973, *M.N.R.A.S.*, **163**, 67.
———. 1976, *Ap. J.*, **203**, 466.
Simon, N. R. 1971, *Ap. J.*, **164**, 331.
———. 1972*a*, *Astr. Ap.*, **21**, 45.
———. 1972*b*, *Astr. Ap.*, **21**, 51.
———. 1976, in *Proceedings of the Solar and Stellar Pulsation Conference*, ed. A. N. Cox and R. G. Deupree (LASL: LA-6544c), p. 173.
Simon, N. R., and Sastri, V. K. 1972, *Astr. Ap.*, **21**, 39.
Simon, N. R., and Schmidt, E. G. 1976, *Ap. J.*, **205**, 162 (SS).
Stellingwerf, R. F. 1974, *Ap. J.*, **192**, 139.
Stobie, R. S. 1969*a*, *M.N.R.A.S.*, **144**, 461.
———. 1969*b*, *M.N.R.A.S.*, **144**, 485.
———. 1969*c*, *M.N.R.A.S.*, **144**, 511.
Unno, W. 1965, *Pub. Astr. Soc. Japan*, **17**, 205.

NORMAN R. SIMON: Behlen Laboratory of Physics, University of Nebraska, Lincoln, NE 68588